Visible-Light-Mediated [2+2]-Cycloadditions for the Formation of Azetine-Based Macrocyclic Dimers

Cody H. Ng[1], Scott L. Kim[1], Ilia Kevlishvili[2], Gianmarco G. Terrones[2], Emily R. Wearing[1], Heather J. Kulik[2,3*], Corinna S. Schindler[1*]

[1]Department of Chemistry, University of Michigan, 930 N University Ave, Ann Arbor, MI 48109, United States

[2]Department of Chemical Engineering, Massachusetts Institute of Technology, 77 Massachusetts Ave, Cambridge, MA 02139, United States

[3]Department of Chemistry, Massachusetts Institute of Technology, 77 Massachusetts Ave, Cambridge, MA 02139, United States

ABSTRACT: Macrocyclic dimeric lactones have known pharmacological activities that make them attractive synthetic targets, but typical synthetic strategies employ an iterative strategy to constructing the macrocycle. Herein, we report a visible-light-mediated approach that enables facile access to 1- and 2-azetine-based dimeric lactones of up to 30-membered ring macrocycles. These products are proposed to form via four consecutive triplet energy transfers for 1-azetine dimeric products and two consecutive triplet energy transfers for 2-azetine dimeric products. Computational investigations provide important insights into the mechanism of this reaction, suggesting that an initial intermolecular [2+2]-cycloaddition is preferred under non-standard Curtin-Hammett conditions over the corresponding intramolecular reaction, ultimately enabling an efficient reaction pathway for macrocyclic dimerization.

INTRODUCTION

Four-membered nitrogen-containing heterocycles, azetidines (**1**) and azetines (**2** and **3**), have recently gained interest as building blocks to access new, underexplored biologically active compounds (Fig. 1A). Numerous advancements have been made in recent years for the synthesis and reactivity of azetidines,[1–3] enabling exploration of the pharmacological properties of azetidine-containing scaffolds.[4] In comparison to azetidines, azetines contain a unit of unsaturation that adds additional ring strain, results in lower nitrogen basicity,[5] and can act as a functional handle for further synthetic modification.[6] Azetines have displayed biological relevance, as 2-azetines are present as Dewar isomer intermediates of UV-light-mediated DNA photodegradation[7–9] and as products of the interaction of a bacterial caseinolytic protease (ClpP) inhibitor with a serine residue.[10] Preliminary studies also indicate the anti-cancer properties of aryl-substituted 1-azetines.[5] However, further studies of the potential biological and pharmaceutical applications of azetines have remained limited, largely due to the lack of general and mild synthetic methods for their construction.

Arguably, the most atom economical approach to access azetines relies on either a [2+2]-cycloaddition between alkenes and nitriles to provide 1-azetines (**2**), or alkynes (**4**) and imines (**5**) to give rise to 2-azetines (**3**). However, a long-standing challenge limiting these approaches is competing electrocyclic ring-opening reactions of azetines (**7**) to form azadienes (**8**, Fig. 1B).[11–13] Consequently, there are

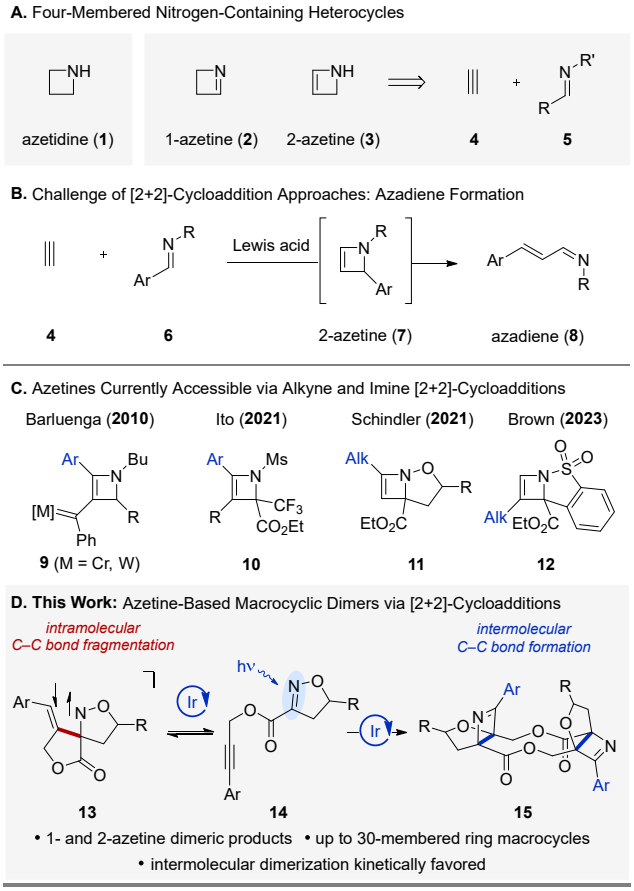

Figure 1. Accessing azetines via [2+2]-cycloaddition.

https://doi.org/10.26434/chemrxiv-2022-h55mx-v2 **ORCID:** https://orcid.org/0000-0003-4968-8013

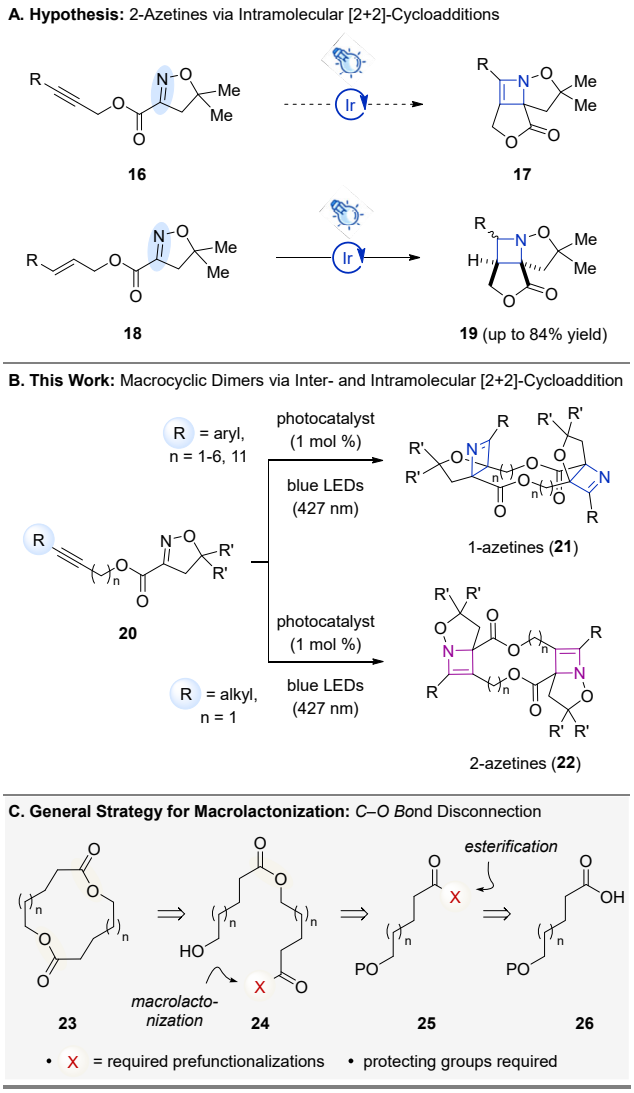

Figure 2. A. Reaction design for formation of tricyclic azetines. **B.** Observed reactivity for 2-isoxazolines containing a tethered alkyne. **C.** General strategy for formation of macrocyclic dimeric lactones.

few successful reports of 1- and 2-azetines accessible via [2+2]-cycloaddition strategies. In 2010, Barluenga and coworkers reported a [2+2]-cycloaddition between alkynylcarbenes and imines for the formation of azetinylcarbenes (**9**, Fig. 1C).[14] More recently, Ito advanced a Lewis acid-catalyzed [2+2]-cycloaddition resulting in the preferred formation of 2-azetines (**10**) over the corresponding unsaturated acyclic imidates.[15] We developed an intermolecular visible-light-mediated [2+2]-cycloaddition between aryl- or alkyl-substituted alkynes and 2-isoxazolines, which provided divergent access to 1- and 2-azetines (**11**) via an energy transfer mechanism.[16] Similarly, Brown reported the formation of 2-azetines (**12**) from alkynes and isothiazole dioxides.[17] Herein, we report a new class of previously inaccessible 1- and 2-azetines (**15**, Fig. 1D). These azetine-based macrocyclic dimeric lactones (**15**) form in a series of consecutive energy transfer events from alkynes **14**. Mechanistic studies suggest a reaction pathway competing with intramolecular cycloaddition (**13**) to ultimately favor intermolecular dimerization and result in up to 30-membered macrocyclic dimeric lactones in a single transformation.

RESULTS AND DISCUSSION

While a photochemical approach to [2+2]-cycloadditions is common, this strategy for azetidines and azetines has been underdeveloped due to challenges associated with the limited photoreactivity of imine precursors.[18] Notably, 2-isoxazolines can overcome these challenges and act as protected imine equivalents in photochemical [2+2]-cycloadditions.[16,19,20] To broaden the scope of accessible azetine products, we envisioned an intramolecular variant of our previously reported transformation,[16] converting 2-isoxazolines (**16**) into the corresponding tricyclic 2-azetines (**17**, Fig. 2A). This strategy was inspired by a recent intramolecular aza Paternò-Büchi reaction developed by our laboratory, in which 2-isoxazolines (**18**) gave rise to tricyclic azetidines (**19**) in up to 84% yield.[20] Herein, we report that instead of an intramolecular [2+2]-cycloaddition to yield monomeric azetines (**17**), 2-isoxazolines (**20**) react under visible-light-mediated energy transfer conditions to form 1- and 2-azetine-based macrocyclic dimers, depending on the choice of alkyne substitution (e.g. aryl or alkyl) (**21** and **22**, Fig. 2B). This divergent reactivity builds on consecutive, independent energy transfer events that rely on an initial intermolecular [2+2]-cycloaddition between two molecules of **20**. Importantly, this new methodology developed offers a new synthetic strategy to access up to 30-membered ring macrocycles in a single transformation from readily accessible substrates.

Macrocycles have displayed impressive potency and selectivity for drug targets, leading to their extensive exploration in drug discovery in recent decades.[21] In comparison to small-molecule drugs, macrocycle drugs can offer advantages of improved binding affinity, selectivity, and oral bioavailability due to their size, structure, and complexity.[22–24] The large size of the macrocycle enables structural pre-organization, in which key binding interactions can occur between the macrocycle and target protein without a significant loss of entropy.[22] Despite their demonstrated utility in drug discovery, the majority of FDA-approved macrocycle therapeutics were inspired by natural products.[21] A limitation to exploration of macrocycles in medicinal chemistry is the lack of robust synthetic strategies to rapidly access macrocycle analogs in a modular fashion. Common synthetic strategies to macrocyclic dimeric lactones involve iterative construction of the acyclic carbon backbone (**24**),[25–37] while ring closure (**23**) typically occurs through *C–O* bond-forming esterification or macrolactonization (Fig. 2C). However, macrolactonization methods require activation of the carboxylic acid precursor (**26**) by using a thioester, mixed anhydride intermediate, or carbodiimide reagent.[38] While isolated examples of direct dimerization of monomeric units exist, these are typically hindered by competing inter- and intramolecular processes,[39–55] resulting in an unmet need for new approaches to access macrocyclic scaffolds. As a solution to this problem, our transformation presents a new method to

Table 1. Optimization of Reaction Conditions

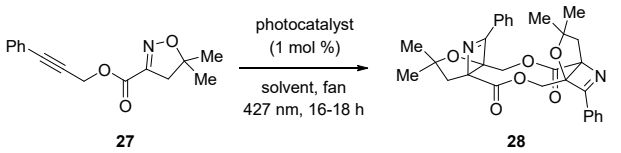

27 **28**

entry	photocatalyst	E_T (kcal·mol^{-1})	solvent	yield (%)	d.r.
1	**Ir1**·PF_6	60.1	MeCN (0.1 M)	64	1.8:1
2	*fac*-[Ir(dFppy)$_3$]	60.1	MeCN (0.1 M)	37	1.6:1
3	2CzPN	60.6	Toluene (0.05 M)	43	3.5:1
4	**Ir2**·PF_6	55.4	MeCN (0.1 M)	51	1.8:1
5	*fac*-[Ir(Fppy)$_3$]	58.6	MeCN (0.1 M)	45	1.7:1
6	**Ir1**·PF_6	60.1	MeCN (0.05 M)	52	1.8:1
7	**Ir1**·PF_6	60.1	MeCN (0.01 M)	36	1.5:1
8	**Ir1**·PF_6	60.1	MeCN (2.5 mM)	21	1.3:1
9	**Ir1**·PF_6	60.1	DCM (0.1 M)	37	2.2:1
10	**Ir1**·PF_6	60.1	THF (0.1 M)	0	-
11	**Ir1**·PF_6	60.1	MeOH (0.1 M)	47	1.8:1
12	**Ir1**·PF_6	60.1	Toluene (0.1 M)	36	2.6:1

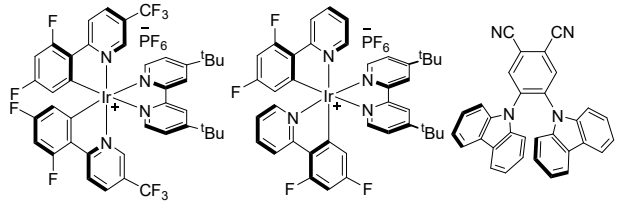

Ir1·PF_6 [Ir(dF(CF_3)ppy)$_2$(dtbbpy)]PF_6 | **Ir2**·PF_6 [Ir(dFppy)$_2$(dtbbpy)]PF_6 | 2CzPN

construct highly complex and unique macrocycles in a modular fashion.

Our studies into the development of this macrocyclic dimerization began with subjecting 2-isoxazoline **27** to conditions previously reported for the intermolecular [2+2]-cycloaddition of 2-isoxazolines and alkynes.[16] Specifically, 1 mol % photocatalyst [Ir(dF(CF_3)ppy)$_2$(dtbbpy)]PF_6 (**Ir1**·PF_6) in 0.1 M acetonitrile provided an initially unexpected product that was ultimately identified as the 1-azetine dimer **28** in 64% yield and 1.8:1 d.r. (Table 1, entry 1). Surveying additional photocatalysts with triplet energies of 55-61 kcal/mol resulted in diminished yields for **28** of 37-51% (entries 2-5). Interestingly, there was no correlation observed between photocatalyst triplet energy and product yield (entries 1-5). The diminished yields from using *fac*-[Ir(dFppy)$_3$], 2CzPN, and *fac*-[Ir(Fppy)$_3$] are likely a result of the strong reducing power ($E_{1/2}^{(M+/M^*)} \leq$ -1.28 V) of these photocatalysts (entries 2, 3, and 5), thus resulting in product decomposition.

We hypothesized that conducting the reaction at lower concentrations could favor the formation of the monomeric 1-azetine that would arise from an intramolecular [2+2]-cycloaddition of **27**.[56] Surprisingly, conducting this reaction at concentrations of 0.05, 0.01, and 0.0025 M resulted in formation of **28** as the major product, albeit in diminished yields (entries 6-8). Final optimization efforts focused on exploring the impact of solvent on product yield and diastereoselectivity. The reaction was found to be compatible with dichloromethane, methanol, and toluene, providing **28** in up to 47% yield (entries 9, 11, and 12). No conversion of **27** was observed in tetrahydrofuran (entry 10). Interestingly, toluene provided **27** in the highest diastereomeric ratios of 3.5:1 and 2.6:1 d.r. (entries 3 and 12). Ultimately, 1 mol % **Ir1**·PF_6 in 0.1 M acetonitrile was selected as the optimal conditions, providing **28** in 64% yield.

Next, the scope of 1-azetine dimeric products was evaluated (Table 2). This reaction was shown to tolerate different aryl and alkyl substitution patterns, linker substitutions, and linker lengths, providing 1-azetine dimers in up to 44% yield and 2-azetine dimers in up to 36% yield. Aryl groups with an electron-withdrawing substituent (**29**) resulted in 44% yield, proving to be superior to unsubstituted aryl groups (**28**, **31**-**32**, **40**-**45**) and aryl groups with an electron-donating substituent (**30**). Increased steric bulk via substitution of the alkyne-ester linker (**31**) proved to hinder reactivity and resulted in 16% yield.[57] Furthermore, **31** was isolated as a mixture of four diastereomers, resulting from the additional stereocenter in the linker.

We next investigated the scope of alkynes bearing aliphatic substituents. Reaction of the methyl-substituted 2-isoxazoline provided the corresponding 2-azetine dimer (**33**) in 41% yield. An increase in yield from 41% to 47% was observed when increasing the reaction concentration to 0.2 M (35% isolated yield, see Supporting Information for more details). Proceeding with these newly optimized conditions, the scope of 2-azetine dimers was subsequently investigated. Ethyl substitution (**34**) provided the product with a comparable yield of 36%. Adding steric bulk to the alkyne resulted in diminished yields, with isopropyl (**35**) and *tert*-butyl groups (**36**) providing the desired products in 19% and 26% yield, respectively. Cyclic alkyl groups (**37**-**39**) were also tolerated in lower yields, resulting in yields of up to 20%.

We were particularly interested in increasing the linker length of the 2-isoxazoline to access larger macrocyclic systems. Importantly, 12-, 14-, and 16-membered macrocycles (**40**-**42**) proved to be readily accessible in up to 28% yield. Furthermore, 18- and 20-membered macrocycles (**43** and **44**) were similarly accessible, albeit in decreased yields of 17% and 13%, respectively. Notably, we were able to isolate a 30-membered macrocycle (**45**) in 10% yield, which demonstrates the utility of this transformation as the dimeric product is the major product observed under the optimal reaction conditions.

Final synthetic efforts were focused on exploring the reactivity of these dimeric products (Fig. 3), as they contain azetine and ester groups that can act as functional handles for further synthetic modification. 1-Azetines are known to be labile under acidic conditions, resulting in ring-opening of the azetine to the corresponding carbonyl and amine.[58] Subjecting **28** to hydrolysis conditions resulted in hydrolysis of both the 1-azetine and ester moieties. Following intramolecular esterification, the [3.3.0] bicyclic lactone **46** was furnished in 23% yield over two steps. This [3.3.0] bicyclic lactone-tetrahydrofuran motif is present in numer-

Table 2. Investigation of substrate scope for 1- and 2-azetine macrocyclic dimers.

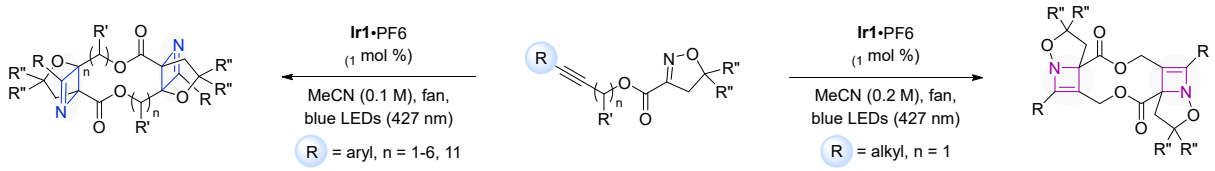

Scope of 1- and 2-Azetine Dimeric Products:

10-membered rings

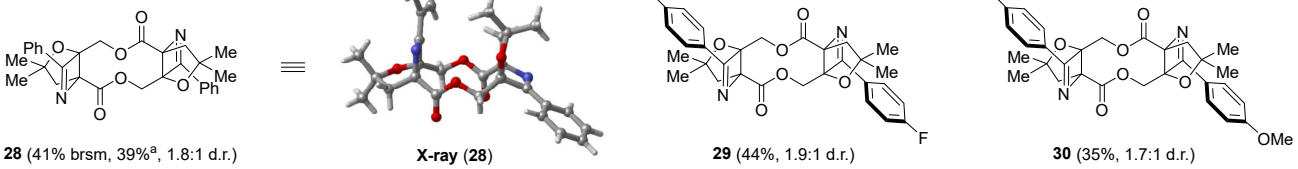

28 (41% brsm, 39%[a], 1.8:1 d.r.)

X-ray (**28**)
major diastereomer

29 (44%, 1.9:1 d.r.)

30 (35%, 1.7:1 d.r.)

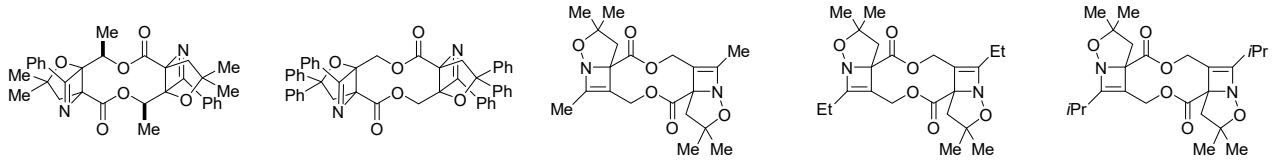

31 (16%, 1:1.1:1.1:1 d.r.)

32 (22%, 3.3:1 d.r.)

33 (35%, 5:1 d.r.[b])

34 (36%, 3.8:1 d.r.)

35 (19%, 3.1:1 d.r.)

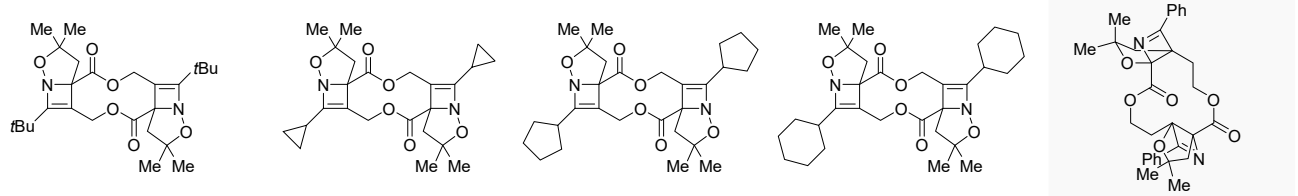

36 (26%, 2.4:1 d.r.)

37 (19%, 2.9:1 d.r.)

38 (16%, 3.6:1 d.r.)

39 (20%, 2.3:1 d.r.)

12-membered ring

40 (12%[c])

14-membered ring

16-membered ring

18-membered ring

20-membered ring

30-membered ring

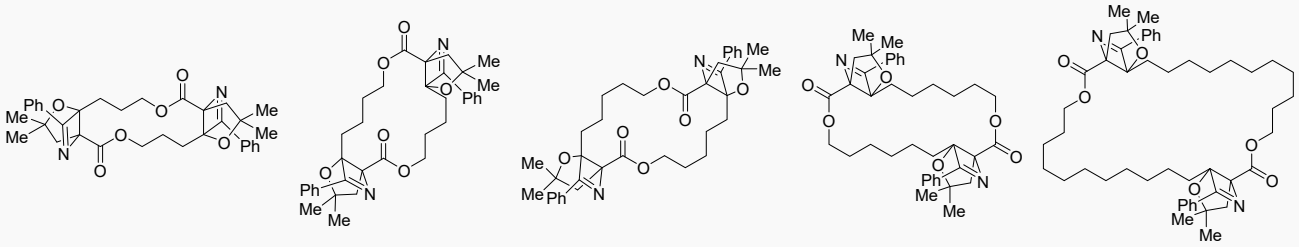

41 (21%, 1.4:1 d.r.)

42 (28%, 1:1 d.r.)

43 (17%, 1.2:1 d.r.)

44 (13%, 1.2:1 d.r.)

45 (10%[c])

ous natural products such as those from the catechin,[59] dehydroaustin,[60] and samaderine[61] families. Interestingly, using $NaBH_3CN$ in MeOH resulted in exclusive opening of the lactone to afford the [3.2.0] bicyclic 1-azetine **47** in 77% yield. Lastly, hydrogenolysis of **28** resulted in the formation of the macrocyclic dimeric lactone **48** in 93% yield.

We proposed the following mechanism for the formation of 1- and 2-azetine dimeric products (Fig. 4). Upon irradiation with visible light, a photoexcited triplet state iridium photocatalyst sensitizes 2-isoxazoline **16** by triplet energy transfer. The resulting triplet state intermediate **I-1** then undergoes an intermolecular [2+2]-cycloaddition with the alkyne moiety of a ground-state molecule of **16** to form intermediate **I-2**. For **I-2** in which R = alkyl, **I-2** is only able to undergo a second energy transfer via sensitization of the 2-isoxazoline, resulting in the triplet state intermediate **I-3**. **I-3** subsequently undergoes an intramolecular [2+2]-cycloaddition to form the 2-azetine dimeric product (**50**). In contrast, for **I-2** in which R = aryl, the styrene moiety is preferentially sensitized to provide the triplet state intermediate **I-4**. This results in rearrangement of **I-4** via *N–O* bond cleavage,[16] intersystem crossing to the corresponding singlet state, and radical combination to the 1-azetine intermediate **I-5**. Upon a third triplet energy transfer to the

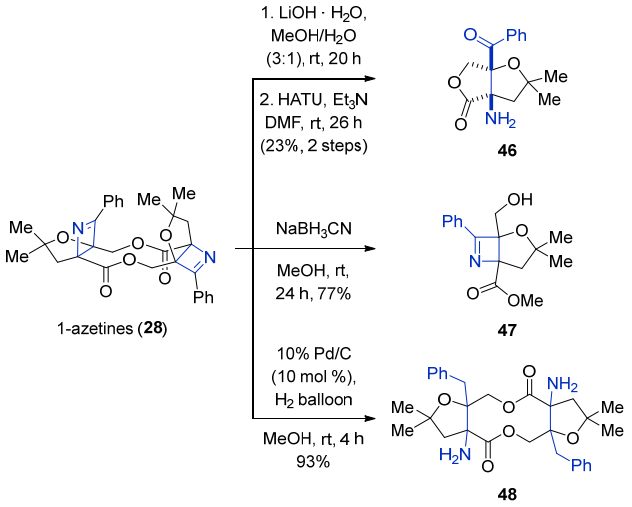

Figure 3. Synthetic modifications of 1-azetine dimeric products.

2-isoxazoline of **I-5**, cyclization occurs via an intramolecular [2+2]-cycloaddition to generate **I-7**. A final sensitization of the styrene moiety of **I-7** and subsequent rearrangement leads to the desired 1-azetine dimeric product (**49**).

Ensuing efforts were focused on performing computational studies using density functional theory (DFT) to gain support for this mechanistic hypothesis. All geometry optimization and frequency calculations were performed using the B3LYP functional with the D4 dispersion correction and the def2-SVP basis set using Orca v. 5.0.1. Single point calculations were carried out using the ωB97X functional with the D4 dispersion correction, def2-TZVPPD basis set and implicit acetonitrile solvent using CPCM. Calculations were consistent with the proposed mechanism: following sensitization of the 2-isoxazoline moiety, the first [2+2]-cycloaddition between $\mathbf{I}^3$ and the alkyne moiety of $\mathbf{I}^1$ occurs through an initial intermolecular *C–C* bond formation ($\mathbf{II}^3$), intersystem crossing ($\mathbf{II}^1$), and radical combination ($\mathbf{III}^1$, Fig. 5A). After the initial *C–C* bond formation step ($\mathbf{TS1}^3$, $\Delta G^{\ddagger}$ = 16.3 kcal/mol), all subsequent transformations to $\mathbf{III}^1$ are near barrierless. Notably, the reverse reaction of $\mathbf{II}^1$ to regenerate starting material $\mathbf{I}^1$ through *C–C* bond fragmentation is disfavored ($\mathbf{TS1}^1$, $\Delta G^{\ddagger}$ = 8.9 kcal/mol). Following formation of $\mathbf{III}^1$, $\mathbf{III}^1$ is then sensitized in a second energy transfer event, allowing for an intramolecular [2+2]-cycloaddition to take place and ultimately result in formation of the final 2-azetine dimerization product $\mathbf{V}^1$.

We next focused on understanding the origin of reactivity differences between alkyl- and aryl-substituted alkyne substrates in time-dependent DFT calculations to analyze the triplet excited states of [2+2]-cycloaddition intermediates (Fig. 5B). Triplet transition energies corresponding to vertical excitation from the ground state and density difference plots both indicate distinct behavior of these two compounds. Energetically, sensitization of the aryl-substi

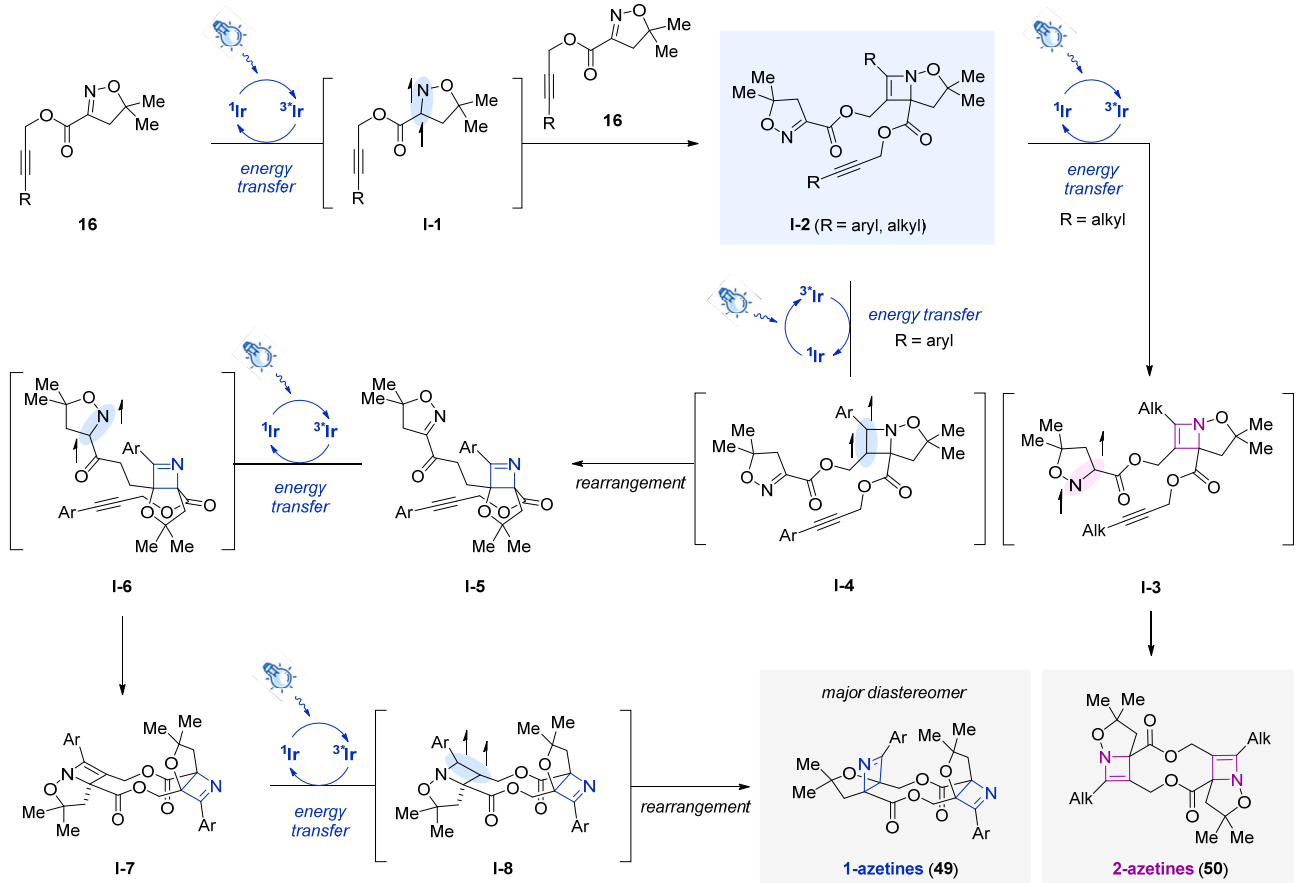

Figure 4. Proposed mechanism for the formation of 1- and 2-azetine dimeric products.

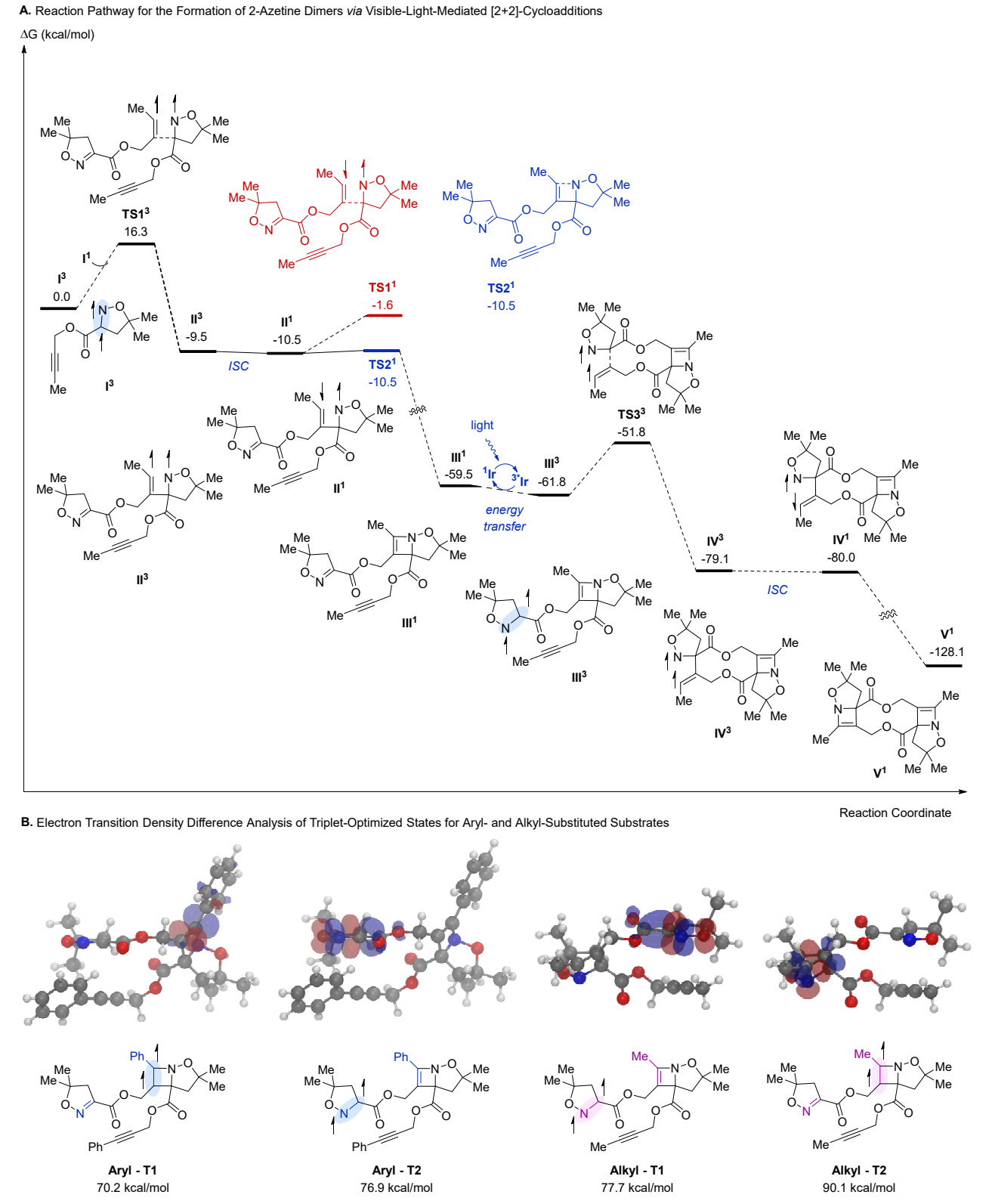

Figure 5. Computational investigations into the proposed mechanism for the formation of 1- and 2-azetine dimeric products. **A.** Intermolecular reaction pathway. An experimental energy of 60.1 kcal/mol was used for the triplet sensitizer to calculate the reaction energy for **III¹** to **III³**. **B.** Transition density difference analysis in triplet excitation shows that in the second energy transfer event, alkene sensitization is preferred for aryl substrates, while oxime sensitization is preferred for alkyl substrates. Density isosurfaces with |0.003| e/bohr³, where blue corresponds to positive phase (triplet), and red corresponds to negative phase (**So**).

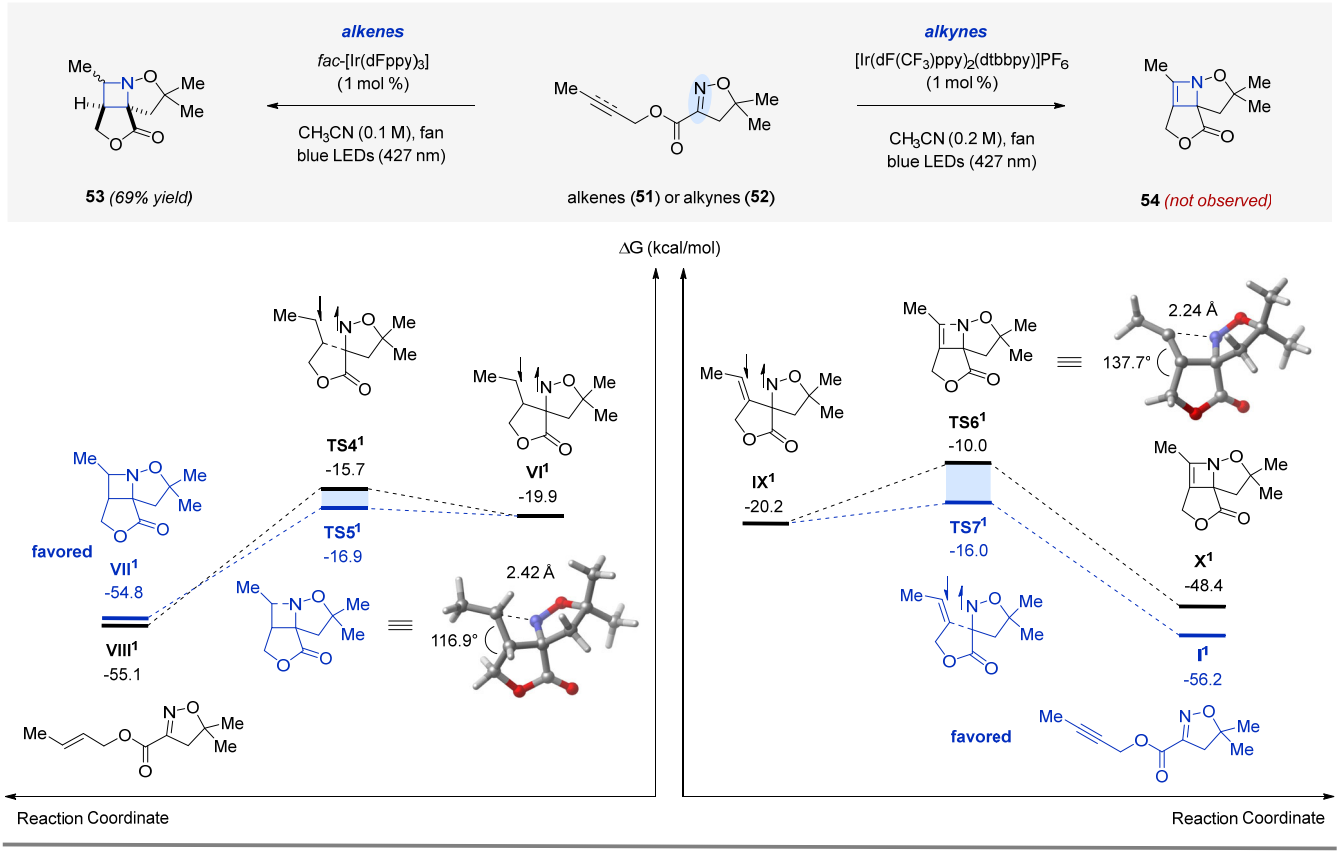

Figure 6. Comparison of the intramolecular pathways towards monomeric products for alkene and alkyne substrates. For alkene substrates, final radical combination to form monomeric azetidines has a low energy barrier. In contrast, for alkyne substrates, monomeric azetines are not kinetically accessible.

tuted intermediate to the first triplet state (**T1**) is more favorable than to the second triplet state (**T2**). Electron density difference analysis, which can show the electron movement from the ground state (**S0**) to the excited state (**T1** or **T2**), indicates that this sensitization involves the styrene moiety, while the second triplet state (**T2**) corresponds to the activated 2-isoxazoline (Fig. 5B). Preferential sensitization of the styrene moiety for aryl-substituted substrates corresponds to experimental observations, as the 1-azetine intermediate (**I-5**, Fig. 4) that arises from styrene sensitization and subsequent *N–O* bond rearrangement has been isolated for select substrates (see Supporting Information for more details). Because the alkyl-substituted substrate does not result in the formation of an intermediate activated alkene, the 2-isoxazoline moiety is sensitized in the first triplet state (**T1**). In contrast, the second triplet state of the alkyl-substituted substrate (**T2**), which involves alkene sensitization, has a significantly higher transition energy. The identity of triplet-optimized states for these two intermediates was also confirmed using spin density analysis on the optimized triplet geometries (Fig. 5B).

With these initial mechanistic results in hand, we subsequently focused on understanding the favored intermolecular reactivity of alkyne substrates **52** leading to macrocyclization, in contrast to the intramolecular reactivity of alkenes **51** (Fig. 6). Specifically, following sensitization of the 2-isoxazoline, initial *C–C* bond formation for the intramolecular reaction pathway is kinetically accessible for both alkyne and alkene substrates, requiring an activation energy of 12.0 and 8.9 kcal/mol, respectively (not shown in Fig. 6, see Supporting Information for more details). *C–C* bond formations for both alkyne and alkene substrates are exergonic by 19.6 and 20.1 kcal/mol, respectively. Following intersystem crossing to the singlet state, the singlet state intermediates (**VI**^{1} and **IX**^{1}) can undergo either a radical combination reaction to form the corresponding azetidine or azetine products, or *C–C* bond cleavage to regenerate the starting material. The barrier for the reverse reaction to reform the starting material for both intermediates is approximately 4 kcal/mol (**TS4**^{1} and **TS7**^{1}). However, the radical combination barrier for forming the azetidine (**VII**^{1}) is only 3.0 kcal/mol (**TS5**^{1}), and azetidine formation is therefore kinetically favored over the reverse reaction on the singlet surface.

In comparison, the barrier for azetine formation (**X**^{1}) is 10.2 kcal/mol (**TS6**^{1}, Fig. 6). The difference in reactivity can be attributed to a significant distortion of the bridging sp^2 carbon, where the highlighted *C–C–C* angle in **TS6**^{1} has a significantly higher strain (137.7°) when compared to the transition state of the alkene analog (**TS4**^{1}, 116.9°). This observation was further confirmed by an intramolecular activation strain model (see Supporting Information for more details), which revealed that both alkyne and linker strain increased by approximately 5 kcal/mol relative to these

groups in the alkene transition state (**TS4**[1]). Therefore, despite a relatively low barrier for the initial *C*–*C* bond formation, the formation of the intramolecular [2+2]-cycloaddition product (**X**[1]) is not accessible due to the reversibility of the *C*–*C* bond adduct on the singlet surface and the increased barrier of the radical combination reaction arising from rigid bridging of the sp^2 carbon center.

Additionally, compared to the activation energy barrier for initial intermolecular *C*–*C* bond formation (**TS1**[3], 16.3 kcal/mol, Fig. 5A), the activation energy for intramolecular *C*–*C* bond formation is lower (12.0 kcal/mol). However, due to the reversibility of the intramolecular intermediate on the singlet surface, this reaction is under non-standard Curtin-Hammett conditions. This indicates that while the intermolecular reaction is kinetically less favorable, the irreversible intermolecular pathway becomes the predominant reaction pathway. The higher barrier for the intermolecular reaction can be primarily attributed to loss of the translational entropy of the bimolecular reaction.

CONCLUSIONS

In conclusion, we report the development of a visible-light-mediated dimerization reaction for 2-isoxazolines containing a tethered alkyne. This unexpected intermolecular [2+2]-cycloaddition outcompetes the initially hypothesized intramolecular reaction pathway under non-standard Curtin-Hammett conditions, enabling a synthetic strategy to access novel products of 1- and 2-azetine-based macrocyclic dimers containing up to a 30-membered ring. Notably, this transformation occurs in one step and deviates from traditional macrolactonization methods. We anticipate that this new method will provide a unique avenue to access biologically interesting synthetic macrocycles. Our mechanistic insights are expected to enable future advances in the development of macrocyclization methodologies.

ASSOCIATED CONTENT

Supporting Information. This material is available free of charge – Experimental procedures, characterization (^{1}H NMR, ^{13}C NMR, IR, and MS data), additional optimization, and control experiments.

Accession Codes. CCDC 2211280 contains the supplementary crystallographic data for this paper. These data can be obtained free of charge via https://www.ccdc.cam.ac.uk/structures/, or by emailing data_request@ccdc.cam.ac.uk, or by contacting The Cambridge Crystallographic Data Centre, 12 Union Road, Cambridge CB2 1EZ, UK; fax: +44 1223 336033.

AUTHOR INFORMATION

Corresponding Author

Heather J. Kulik –Email: hjkulik@mit.edu

Corinna S. Schindler –Email: corinnas@umich.edu

Author Contributions

The manuscript was written through contributions of all authors. All authors have given approval to the final version of the manuscript.

Notes

The authors declare no competing financial interest.

ACKNOWLEDGMENT

This work was supported by the NSF Center for the Chemistry of Molecularly Optimized Networks (MONET; Award CHE2116298) for personnel and by the NIH (R01-GM141340) for the cost of chemicals and consumables. C.H.N. thanks the NSF for a Predoctoral Fellowship. E.R.W. thanks the NSF for a Predoctoral Fellowship and the University of Michigan Rackham Graduate School for a Predoctoral Fellowship. We thank Dr. Fengrui Qu for performing X-ray crystallography and Dr. Russell Bornschein for performing mass spectrometry.

REFERENCES

(1) Brandi, A.; Cicchi, S.; Cordero, F. M. Novel Syntheses of Azetidines and Azetidinones. Chem. Rev. 2008, 108 (9), 3988–4035. https://doi.org/10.1021/cr800325e.

(2) Richardson, A. D.; Becker, M. R.; Schindler, C. S. Synthesis of Azetidines by Aza Paternò–Büchi Reactions. Chem. Sci. 2020, 11 (29), 7553–7561. https://doi.org/10.1039/D0SC01017K.

(3) Mughal, H.; Szostak, M. Recent Advances in the Synthesis and Reactivity of Azetidines: Strain-Driven Character of the Four-Membered Heterocycle. Org. Biomol. Chem. 2021, 19 (15), 3274–3286. https://doi.org/10.1039/D1OB00061F.

(4) Parmar, D. R.; Soni, J. Y.; Guduru, R.; Rayani, R. H.; Kusurkar, R. V.; Vala, A. G. Azetidines of Pharmacological Interest. Arch Pharm 2021, 354 (11), 2100062. https://doi.org/10.1002/ardp.202100062.

(5) Smetanin, I. A.; Novikov, M. S.; Agafonova, A. V.; Rostovskii, N. V.; Khlebnikov, A. F.; Kudryavtsev, I. V.; Terpilowski, M. A.; Serebriakova, M. K.; Trulioff, A. S.; Goncharov, N. V. A Novel Strategy for the Synthesis of Thermally Stable and Apoptosis-Inducing 2,3-Dihydroazetes. Org. Biomol. Chem. 2016, 14 (19), 4479–4487. https://doi.org/10.1039/C6OB00588H.

(6) Gatazka, M. R.; McFee, E. C.; Ng, C. H.; Wearing, E. R.; Schindler, C. S. New Strategies for the Synthesis of 1- and 2-Azetines and Their Applications as Value-Added Building Blocks. Org. Biomol. Chem. 2022, 20 (46), 9052–9068. https://doi.org/10.1039/D2OB01812H.

(7) Taylor, J. S.; Cohrs, M. P. DNA, Light, and Dewar Pyrimidinones: The Structure and Biological Significance to TpT3. J. Am. Chem. Soc. 1987, 109 (9), 2834–2835. https://doi.org/10.1021/ja00243a052.

(8) Douki, T.; Rebelo-Moreira, S.; Hamon, N.; Bayle, P.-A. DNA Photochemistry: Geometrically Unconstrained Pyrimidine (6–4) Pyrimidone Photoproducts Do Photoisomerize. Org. Lett. 2015, 17 (2), 246–249. https://doi.org/10.1021/ol5033267.

(9) Douki, T.; Sage, E. Dewar Valence Isomers, the Third Type of Environmentally Relevant DNA Photoproducts Induced by Solar Radiation. Photochem Photobiol Sci 2016, 15 (1), 24–30. https://doi.org/10.1039/c5pp00382b.

(10) Culp, E. J.; Sychantha, D.; Hobson, C.; Pawlowski, A. C.; Prehna, G.; Wright, G. D. ClpP Inhibitors Are Produced by a Widespread Family of Bacterial Gene Clusters. Nat Microbiol 2022, 7 (3), 451–462. https://doi.org/10.1038/s41564-022-01073-4.

(11) Ishitani, H.; Nagayama, S.; Kobayashi, S. A New Reaction of Imines with Alkynyl Sulfides Affording α,β-Unsaturated Thioimidates. J. Org. Chem. 1996, 61 (6), 1902–1903. https://doi.org/10.1021/jo9519241.

(12) Ma, Y.; Qian, C. [2+2] Cycloaddition Reactions of Imines with Alkynyl Selenides Catalyzed by Scandium Triflate. Tetrahedron Letters 2000, 41 (6), 945–947. https://doi.org/10.1016/S0040-4039(99)02178-4.

(13) Lopez, S. A.; Houk, K. N. Substituent Effects on Rates and Torquoselectivities of Electrocyclic Ring-Openings of N -Substituted 2-Azetines. J. Org. Chem. 2014, 79 (13), 6189–6195. https://doi.org/10.1021/jo500919s.

(14) Barluenga, J.; Gómez, A.; Santamaría, J.; Tomás, M. Sequential Five-Component Construction of the Cyclopenta[e][1,3]Oxazine Skeleton Using Stable 2-Azetine Derivatives. Angewandte Chemie International Edition 2010, 49 (7), 1306–1308. https://doi.org/10.1002/anie.200906357.

(15) Hara, S.; Ito, S. TiCl 4 -Mediated [2+2] Cycloaddition for Synthesis of Isolable CF 3 -Substituted 2-Azetines. Asian J of Organic Chemis 2021, 10 (4), 788–792. https://doi.org/10.1002/ajoc.202100082.

(16) Wearing, E. R.; Blackmun, D. E.; Becker, M. R.; Schindler, C. S. 1- and 2-Azetines via Visible Light-Mediated [2 + 2]-Cycloadditions of Alkynes and Oximes. J. Am. Chem. Soc. 2021, 143 (39), 16235–16242. https://doi.org/10.1021/jacs.1c07523.

(17) Wang, W.; Brown, M. K. Photosensitized [4+2]- and [2+2]-Cycloaddition Reactions of N -Sulfonylimines. Angew Chem Int Ed 2023, e202305622. https://doi.org/10.1002/anie.202305622.

(18) Kandappa, S. K.; Valloli, L. K.; Ahuja, S.; Parthiban, J.; Sivaguru, J. Taming the Excited State Reactivity of Imines – from Non-Radiative Decay to Aza Paternò–Büchi Reaction. Chem. Soc. Rev. 2021, 50 (3), 1617–1641. https://doi.org/10.1039/D0CS00717J.

(19) Becker, M. R.; Wearing, E. R.; Schindler, C. S. Synthesis of Azetidines via Visible-Light-Mediated Intermolecular [2+2] Photocycloadditions. Nat. Chem. 2020, 12 (10), 898–905. https://doi.org/10.1038/s41557-020-0541-1.

(20) Blackmun, D. E.; Chamness, S. A.; Schindler, C. S. Intramolecular, Visible-Light-Mediated Aza Paternò-Büchi Reactions of Unactivated Alkenes. Org. Lett. 2022, acs.orglett.2c01008. https://doi.org/10.1021/acs.orglett.2c01008.

(21) Garcia Jimenez, D.; Poongavanam, V.; Kihlberg, J. Macrocycles in Drug Discovery—Learning from the Past for the Future. J. Med. Chem. 2023, acs.jmedchem.3c00134. https://doi.org/10.1021/acs.jmedchem.3c00134.

(22) Driggers, E. M.; Hale, S. P.; Lee, J.; Terrett, N. K. The Exploration of Macrocycles for Drug Discovery — an Underexploited Structural Class. Nat Rev Drug Discov 2008, 7 (7), 608–624. https://doi.org/10.1038/nrd2590.

(23) Marsault, E.; Peterson, M. L. Macrocycles Are Great Cycles: Applications, Opportunities, and Challenges of Synthetic Macrocycles in Drug Discovery. J. Med. Chem. 2011, 54 (7), 1961–2004. https://doi.org/10.1021/jm1012374.

(24) Giordanetto, F.; Kihlberg, J. Macrocyclic Drugs and Clinical Candidates: What Can Medicinal Chemists Learn from Their Properties? J. Med. Chem. 2014, 57 (2), 278–295. https://doi.org/10.1021/jm400887j.

(25) Colvin, E. W.; Purcell, T. A.; Raphael, R. A. Total Synthesis of the Macrocyclic Antibiotic (±)-Pyrenophorin. J. Chem. Soc., Perkin Trans. 1 1976, No. 16, 1718–1722. https://doi.org/10.1039/P19760001718.

(26) Fukuyama, Y.; Kirkemo, C. L.; White, J. D. A Novel Synthesis of (.+-.)-Vermiculine. J. Am. Chem. Soc. 1977, 99 (2), 646–647. https://doi.org/10.1021/ja00444a073.

(27) Noda, A.; Aoyagi, S.; Machinaga, N.; Kibayashi, C. Total Synthesis of (–)-Vermiculine. Tetrahedron Letters 1994, 35 (44), 8237–8240. https://doi.org/10.1016/0040-4039(94)88291-6.

(28) Hillier, M. C.; Price, A. T.; Meyers, A. I. Studies on the Total Synthesis of Disorazole C 1 . An Advanced Macrocycle Intermediate. J. Org. Chem. 2001, 66 (18), 6037–6045. https://doi.org/10.1021/jo010249e.

(29) Soltani, O.; De Brabander, J. K. A Concise Synthesis of (+)-SCH 351448. Org. Lett. 2005, 7 (13), 2791–2793. https://doi.org/10.1021/ol0510769.

(30) Nicolaou, K. C.; Nold, A. L.; Milburn, R. R.; Schindler, C. S.; Cole, K. P.; Yamaguchi, J. Total Synthesis of Marinomycins A–C and of Their Monomeric Counterparts Monomarinomycin A and Iso -Monomarinomycin A. J. Am. Chem. Soc. 2007, 129 (6), 1760–1768. https://doi.org/10.1021/ja068053p.

(31) Gutiérrez, M.; Andrianasolo, E. H.; Shin, W. K.; Goeger, D. E.; Yokochi, A.; Schemies, J.; Jung, M.; France, D.; Cornell-Kennon, S.; Lee, E.; Gerwick, W. H. Structural and Synthetic Investigations of Tanikolide Dimer, a SIRT2 Selective Inhibitor, and Tanikolide Seco -Acid from the Madagascar Marine Cyanobacterium Lyngbya Majuscula. J. Org. Chem. 2009, 74 (15), 5267–5275.

(32) Zhu, K.; Panek, J. S. Total Synthesis of (+)-SCH 351448. Org. Lett. 2011, 13 (17), 4652–4655. https://doi.org/10.1021/ol201863b.

(33) Dieckmann, M.; Rudolph, S.; Dreisigacker, S.; Menche, D. Concise Synthesis of the Macrocyclic Core of Rhizopodin by a Heck Macrocyclization Strategy. J. Org. Chem. 2012, 77 (23), 10782–10788. https://doi.org/10.1021/jo302134y.

(34) Evans, P. A.; Huang, M.-H.; Lawler, M. J.; Maroto, S. Total Synthesis of Marinomycin A Using Salicylate as a Molecular Switch to Mediate Dimerization. Nature Chem 2012, 4 (8), 680–684. https://doi.org/10.1038/nchem.1330.

(35) Dalby, S. M.; Goodwin-Tindall, J.; Paterson, I. Total Synthesis of (–)-Rhizopodin. Angew. Chem. Int. Ed. 2013, 52 (25), 6517–6521. https://doi.org/10.1002/anie.201301978.

(36) Nabika, R.; Oishi, S.; Misu, R.; Ohno, H.; Fujii, N. Synthesis of IB-01212 by Multiple N-Methylations of Peptide Bonds. Bioorganic & Medicinal Chemistry 2014, 22 (21), 6156–6162. https://doi.org/10.1016/j.bmc.2014.08.036.

(37) Wang, G.; Krische, M. J. Total Synthesis of (+)-SCH 351448: Efficiency via Chemoselectivity and Redox-Economy Powered by Metal Catalysis. J. Am. Chem. Soc. 2016, 138 (26), 8088–8091. https://doi.org/10.1021/jacs.6b04917.

(38) Parenty, A.; Moreau, X.; Niel, G.; Campagne, J.-M. Update 1 of: Macrolactonizations in the Total Synthesis of Natural Products. Chem. Rev. 2013, 113 (1), PR1–PR40. https://doi.org/10.1021/cr300129n.

(39) Corey, E. J.; Nicolaou, K. C.; Melvin, L. S. Synthesis of Brefeldin A, Carpaine, Vertaline, and Erythronolide B from Nonmacrocyclic Precursors. J. Am. Chem. Soc. 1975, 97 (3), 654–655. https://doi.org/10.1021/ja00836a037.

(40) Corey, E. J.; Nicolaou, K. C.; Toru, T. Total Synthesis of (+-)-Vermiculine. J. Am. Chem. Soc. 1975, 97 (8), 2287–2288. https://doi.org/10.1021/ja00841a058.

(41) Sato, T.; Aoyagi, S.; Kibayashi, C. Enantioselective Total Synthesis of (+)-Azimine and (+)-Carpaine. Org. Lett. 2003, 5 (21), 3839–3842. https://doi.org/10.1021/ol030088w.

(42) Gogoi, S.; Barua, N. C.; Kalita, B. First Total Synthesis of Verbalactone, a Macrocyclic Dilactone Isolated from Verbascum Undulatum. Tetrahedron Letters 2004, 45 (29), 5577–5579. https://doi.org/10.1016/j.tetlet.2004.05.149.

(43) Allais, F.; Louvel, M.-C.; Cossy, J. A Short and Highly Diastereoselective Synthesis of Verbalactone. Synlett 2007, 2007 (3), 0451–0452. https://doi.org/10.1055/s-2007-967946.

(44) Gesinski, M. R.; Rychnovsky, S. D. Total Synthesis of the Cyanolide A Aglycon. J. Am. Chem. Soc. 2011, 133 (25), 9727–9729. https://doi.org/10.1021/ja204228q.
(45) Nishimaru, T.; Kondo, M.; Takeshita, K.; Takahashi, K.; Ishihara, J.; Hatakeyama, S. Total Synthesis of Marinomycin A Based on a Direct Dimerization Strategy. Angew. Chem. Int. Ed. 2014, 53 (32), 8459–8462. https://doi.org/10.1002/anie.201404408.
(46) Gunasekera, S. P.; Li, Y.; Ratnayake, R.; Luo, D.; Lo, J.; Reibenspies, J. H.; Xu, Z.; Clare-Salzler, M. J.; Ye, T.; Paul, V. J.; Luesch, H. Discovery, Total Synthesis and Key Structural Elements for the Immunosuppressive Activity of Cocosolide, a Symmetrical Glycosylated Macrolide Dimer from Marine Cyanobacteria. Chem. Eur. J. 2016, 22 (24), 8158–8166. https://doi.org/10.1002/chem.201600674.
(47) Nicolaou, K. C.; Pulukuri, K. K.; Rigol, S.; Peitsinis, Z.; Yu, R.; Kishigami, S.; Cen, N.; Aujay, M.; Sandoval, J.; Zepeda, N.; Gavrilyuk, J. Short Total Synthesis of Δ 12 -Prostaglandin J 2 and Related Prostaglandins. Design, Synthesis, and Biological Evaluation of Macrocyclic Δ 12 -Prostaglandin J 2 Analogues. J. Org. Chem. 2019, 84 (1), 365–378. https://doi.org/10.1021/acs.joc.8b03057.
(48) Kruizinga, W. H.; Kellogg, R. M. Preparation of Macrocyclic Lactones by Ring Closure of Cesium Carboxylates. J. Am. Chem. Soc. 1981, 103 (17), 5183–5189. https://doi.org/10.1021/ja00407a039.
(49) Scott, P. W.; Harrison, I. T.; Bittner, S. Preparation of Macrocyclic Lactones from Cyclohexane-1,3-Diones. J. Org. Chem. 1981, 46 (9), 1914–1915. https://doi.org/10.1021/jo00322a035.
(50) Chen, C.; Quinn, E. K.; Olmstead, M. M.; Kurth, M. J. Thermal Cycloreversion of 2,2-Dimethyl-6 (.Omega.-Hydroxyalkyl)-4H-1,3-Dioxin-4-Ones: Mono-, Di-, and Trimeric Macrocyclic .Beta.-Keto Lactones by Intramolecular Trapping of (.Omega.-Hydroxy)Acylketenes. J. Org. Chem. 1993, 58 (18), 5011–5014. https://doi.org/10.1021/jo00070a047.
(51) Shibuya, H.; Ohashi, K.; Narita, N.; Hori, K.; Kawanishi, H.; Ishida, T.; Kitagawa, I. Chemical Transformation of Terpenoids. IX. Ionophoretic Activities of Macrocyclic Lactone Epoxides Synthesized from E,E-Farnesol. Chem. Pharm. Bull. 1993, 41 (12), 2113–2120. https://doi.org/10.1248/cpb.41.2113.
(52) Shibuya, H.; Ohashi, K.; Narita, N.; Ishida, T.; Kitagawa, I. Chemical Transformation of Terpenoids. X. Ionophoretic Activities of Macrocyclic Lactone Epoxides Synthesized from Geraniol. Chem. Pharm. Bull. 1994, 42 (2), 293–299. https://doi.org/10.1248/cpb.42.293.
(53) Lee, C. W.; Grubbs, R. H. Formation of Macrocycles via Ring-Closing Olefin Metathesis. J. Org. Chem. 2001, 66 (21), 7155–7158. https://doi.org/10.1021/jo0158480.
(54) Gesinski, M. R.; Tadpetch, K.; Rychnovsky, S. D. Symmetric Macrocycles by a Prins Dimerization and Macrocyclization Strategy. Org. Lett. 2009, 11 (22), 5342–5345. https://doi.org/10.1021/ol9022062.
(55) For the formation of a 12-membered dimeric lactone via a Paternò-Büchi approach, see: Arimura, J.; Mizuta, T.; Hiraga, Y.; Abe, M. Formation of Macrocyclic Lactones in the Paternò–Büchi Dimerization Reaction. Beilstein J. Org. Chem. 2011, 7, 265–269. https://doi.org/10.3762/bjoc.7.35.
(56) In Reference (20), This Strategy Addressed Competing Intermolecular Reaction Pathways and Resulted in Significantly Improved Yields for Low-Yielding Substrates.
(57) The Diminished Yield of 28 Could Be Due to the Thorpe-Ingold Effect, Which Would Typically Favor Intramolecular Cyclization. However, We Did Not Observe the Tricyclic Azetine Product under These Conditions Because the Intramolecular Pathway of This Reaction Leads to Reforming the Starting Material under Non-Standard Curtin-Hammett Conditions.
(58) Pifferi, G.; Consonni, P.; Pelizza, G.; Testa, E. 1-Azetines. Journal of Heterocyclic Chemistry 1967, 4 (4), 619–624. https://doi.org/10.1002/jhet.5570040426.
(59) Hashimoto, F.; Nonaka, G.; Nishioka, I. Tannins and Related Compounds. XC. 8-C-Ascorbyl (-)-Epigallocatechin 3-O-Gallate and Novel Dimeric Flavan-3-Ols, Oolong-homobisflavans A and B, from Oolong Tea.(3). Chem. Pharm. Bull. 1989, 37 (12), 3255–3263. https://doi.org/10.1248/cpb.37.3255.
(60) Santos, R. M. G. D.; Rodrigues-Filho, E. Structures of Meroterpenes Produced by Penicillium Sp, an Endophytic Fungus Found Associated with Melia Azedarach. J. Braz. Chem. Soc. 2003, 14 (5), 722–727. https://doi.org/10.1590/S0103-50532003000500004.
(61) Kitagawa, I.; Mahmud, T.; Yokota, K.; Nakagawa, S.; Mayumi, T.; Kobayashi, M.; Shibuya, H. Indonesian Medicinal Plants. XVII. Characterization of Quassinoids from the Stems of Quassia Indica. Chem. Pharm. Bull. 1996, 44 (11), 2009–2014. https://doi.org/10.1248/cpb.44.2009.